© 2002 The Chemical Society of Japan Bull. Chem. Soc. Jpn., 75, 2609–2614 (2002) 2609

Polymeric Manganese Carboxylato Compounds $[\{Mn[m\text{-}C_6H_4(COO)_2](C_5H_5N)_2\}_n]$ and $[\{Mn(3\text{-}C_5H_4NCOO)_2\}_n]$ with One- and Three-Dimensional Extended Structures

Wenguo Wang,[#] Chengbing Ma, Xiaofeng Zhang, Changneng Chen, Qiutian Liu,[*] Feng Chen, Daizheng Liao,[†] and Licun Li[†]

State Key Laboratory of Structural Chemistry, Fujian Institute of Research on the Structure of Matter, Chinese Academy of Sciences, Fuzhou, Fujian 350002, China

†Department of Chemistry, Nankai University, Tianjing 300071, China

(Received May 27, 2002)

Two catena manganese carboxylato complexes $[\{Mn[m\text{-}C_6H_4(COO)_2](C_5H_5N)_2\}_n]$ (**1**) and $[\{Mn(3\text{-}C_5H_4NCOO)_2\}_n]$ (**2**) were synthesized and structurally characterized. Isophthalate together with pyridine as a capping ligand leads to a 1-D alternating chain structure of complex **1**, while 3-pyridinecarboxylate (also known as nicotinate) results in a 3-D network of complex **2**, implying an effect of the ligand on the dimensionality of the extended structure. Stretching vibration differences, $\Delta(\nu_{as}-\nu_s) < 200\ \mathrm{cm^{-1}}$, for the COO^- groups of both complexes were observed to be consistent with the bridging and chelating coordination modes. The variable-temperature conductance of **1** displays a semiconductor feature. Magnetic exchange interactions were analyzed using models composed of $Mn_2(\mu\text{-}COO)_2$ and $Mn_2(\mu\text{-acidate})_2$ moieties, exhibiting an antiferromagnetic coupling behavior for each complex through $Mn_2(\mu\text{-}COO)_2$ moieties. The magnetic interaction in the $Mn_2(\mu\text{-acidate})_2$ moieties is negligible.

Carboxylate as a versatile ligand has recently attracted more attention in coordination chemistry. Polynuclear metal carboxylates have been used to explore exchange coupling interactions between adjacent metal ions.[1] Metal complexes with extended structures have attracted great interest in studies of magnetically coupling because of promising applications in the field of molecular magnetism. Carboxylate connects paramagnetic centers to build a spatially well-spanned framework by various bridging modes, and mediates superexchange interactions between the paramagnetic centers. The chemistry of manganese has been especially well developed in recent years because manganese is catalytically active in a variety of metalloenzymes.[2] Poly(manganese carboxylate) complexes[3] have become an important research field for the simulation of relevant manganese enzymes and the exploration of magnetism. Phthalates have two *p*-, *m*-, or *o*-carboxylato groups which link manganese sites in diversified modes, resulting in a series of phthalato manganese polymers.[4] It is interesting that *m*- and *o*-phthalato manganese complexes have a one-dimensional (1-D) extended structure, while terephthalato complexes have a three-dimensional (3-D) structure.[4b,c] It is comprehensible that the largest separation between both *p*-carboxylato groups lowers the crowding of the groups and, therefore, terephthalate would be favorable to simultaneously connect with more Mn ions to construct a network structure. The control of dimensionality has become a major challenge for the rational design of molecular architecture. To our knowledge, catena manganese complexes possessing multidimensional extended structures are still rare.[5] In this work we report on a preliminary attempt to control the dimensionality of the extended structure for the manganese complex. Isophthalic acid and pyridine mixed ligands were used to build a one-dimensional manganese complex $[\{Mn(m\text{-phth})(py)_2\}_n]$ (**1**, py = pyridine; phth = phthalate), while 3-pyridinecarboxylic acid was used to produce a 3-D manganese complex $[\{Mn(3\text{-}C_5H_4NCOO)_2\}_n]$ (**2**).

Results and Discussion

Complex **1** was synthesized in a $MeOH/H_2O$ solution at reflux temperature. The coordination sphere of Mn in **1** shown in Fig. 1 is a distorted octahedron with two N atoms of pyridine located at opposed positions with N–Mn–N angle of 168.44(8)°. Selected bond lengths and angles are listed in Table 1. It is noted that when compared to the shorter Mn–O3A and Mn–O4B bonds, carboxyl chelating Mn–O1and Mn–O2 bonds are lengthened to 2.2480(17) and 2.2871(18) Å owing to an astriction of the chelating angle (58.08(6)°). Pyridine caps the manganese site, forming the $(py)_2Mn$ moiety, which is alternately linked by double μ-COO and double μ-isophthalate bridges to make a 1-D alternating chain as shown in Fig. 1 with Mn···Mn separations of 4.582 Å and 7.024 Å, respectively. This feature is different from that of the other isophthalate manganese complex, $[\{Mn_2(m\text{-phth})(phen)_4\}_n](ClO_4)_{2n}$[4e] (phen = 1,10-phenanthroline), which contains $(phen)_2Mn$ moieties linked by single μ-isophthalate bridges to form a zigzag 1-D chain. The existence of capping ligands (py and phen)

[#] Graduate School of the Chinese Academy of Sciences, Beijing, China in the Mn(II) coordination spheres of these two complexes may block the way towards a 3-D structure. N-containing ligands, such as phen, N_2O_2 Schiff base and so on, were generally involved in the Mn(II) coordination sphere to construct independent Mn/N moieties by chelation of the ligand to the manganese atom, while the phthalate ligands link these Mn/N moieties to result in 1-D chains. The amount of chelating donor atoms may cause a variation of the chain structure as shown in Scheme 1. Schiff base (N_2O_2 4 donor atoms) and phen (2 donor atoms) engender single μ-phthalate[4e,g] or single μ-COO bridges[4d] between the two Mn/N moieties, while pyridine containing only one donor atom brings double bridges in complex **1**. Nicotinate ligand possesses both carboxyl and an N donor at the *meta*-position, which is difficult to chelate to the manganese atom by N and O donors, and is able to coordinate simultaneously to three manganese ions in various directions and to unlimitedly extend these coordination bonds. It is expected that nicotinate would be favorable to construct 3-D network of the manganese complexes, though only a complex $[\{(H_2O)_2Mn(3\text{-}C_5H_4NCOO)_2\}_n]$ with 2-D layer structure and $(H_2O)_2Mn$ capping moieties has been reported.[6] We adopted hydrothermal method instead of the conventional method to enhance the chance of the ligands contacting to the Mn(II) ion. Complex **2** was hydrothermally synthesized by heating $MnCl_2{\cdot}4H_2O$ and nicotinic acid in a mole ratio of 1:2.8. In the structure of **2** shown in Fig. 2, the Mn(II) ion locates on a 2-fold axis and is coordinated by six nicotinate ligands, forming a distorted octahedral sphere with the axial O–Mn–N(or O) angles ranging from 165.86(13)° to 172.06(9)° and the other angles of 84.86(9)°–100.76(14)°. Selected bond distances and angles are also given in Table 1. Two types of moieties were observed, one of which is $Mn_2(\mu\text{-COO})_2$ with the shortest Mn···Mn separation of 4.917 Å, the other is $Mn_2(\mu\text{-nicotinate-N,O})_2$ with Mn···Mn separation of 7.342 Å. The $Mn_2(\mu\text{-COO})_2$ moiety forms 8 atomic plane with the largest deviation of ±0.168 Å; the $Mn_2(\mu\text{-nicotinate-N,O})_2$ moiety contains 12 atomic plane consisting of 2Mn, 2N, 2O and 6C atoms with the

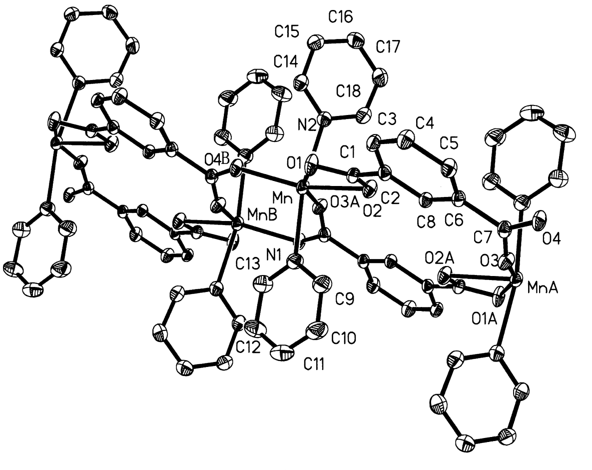

Fig. 1. ORTEP diagram of **1** showing the atom-numbering scheme of a $Mn(m\text{-phth})(py)_2$ moiety and thermal ellipsoids at 30% probability. $Mn_2(\mu\text{-CO}_2)_2$ and $Mn_2(\mu\text{-isophthalate})_2$ moieties alternately link to form one-dimensional chain of complex **1**.

Table 1. Selected Bond Lengths [Å] and Angles [°] for Complexes **1** and **2**

	1[a)]		
Mn–O4B	2.1115(18)	Mn–O3A	2.1194(17)
Mn–O2	2.2480(17)	Mn–O1	2.2871(18)
Mn–N2	2.295(2)	Mn–N1	2.307(2)
O4B–Mn–O3A	105.48(7)	O4B–Mn–N2	90.45(7)
O4B–Mn–O2	152.45(7)	O3A–Mn–N2	84.90(7)
O3A–Mn–O2	101.05(7)	O2–Mn–N2	84.58(7)
O4B–Mn–O1	94.96(6)	O1–Mn–N2	90.20(7)
O3A–Mn–O1	158.99(7)	O4B–Mn–N1	100.42(8)
O2–Mn–O1	58.08(6)	O3A–Mn–N1	88.38(7)
O2–Mn–N1	87.50(7)	O1–Mn–N1	92.74(8)
N2–Mn–N1	168.44(8)		
	2[b)]		
Mn–O1C	2.125(2)	Mn–O1B	2.125(2)
Mn–O2E	2.197(2)	Mn–O2D	2.197(2)
Mn–N	2.356(3)	Mn–NA	2.356(3)
O1C–Mn–O1B	87.75(14)	O2D–Mn–N	84.86(9)
O1C–Mn–O2E	99.98(9)	O1C–Mn–NA	172.06(9)
O1B–Mn–O2E	90.23(9)	O1B–Mn–NA	85.93(10)
O1C–Mn–O2D	90.23(9)	O2E–Mn–NA	84.86(9)
O1B–Mn–O2D	99.98(9)	O2D–Mn–NA	86.14(9)
O2E–Mn–O2D	165.86(13)	N–Mn–NA	100.76(14)
O1C–Mn–N	85.93(10)	O1B–Mn–N	172.06(9)
O2E–Mn–N	86.14(9)		

a) Symmetry transformations: A: $-x+1$, $-y$, $-z+1$; B: x, y, $z+1$. b) Symmetry transformations: A, $-x+1$, y, $-z+1/2$; B, $x-1/2$, $y+1/2$, z; C, $-x+3/2$, $y+1/2$, $-z+1/2$; D, $-x+3/2$, $-y+1/2$, $-z+1$; E, $x-1/2$, $-y+1/2$, $z-1/2$.

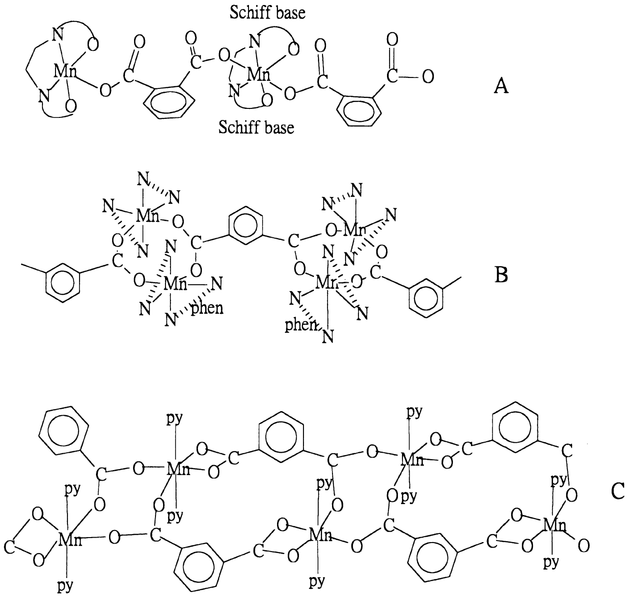

Scheme 1. (A) Single phthalate bridges between Mn moieties of N_2O_2 Schiff base. (B) Single phthalate bridges between $(phen)_2Mn$ moieties. (C) Double phthalate bridges between $(py)_2Mn$ moieties.

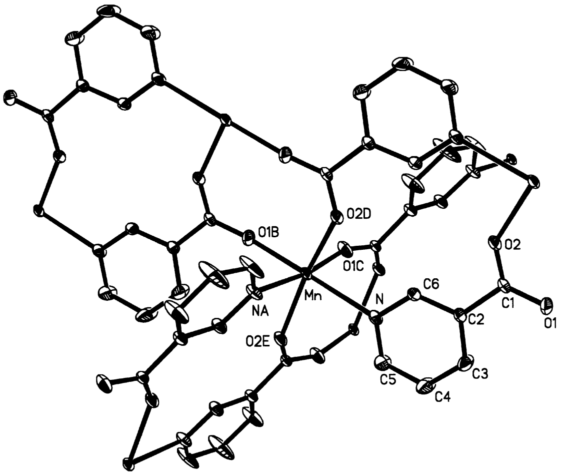

Fig. 2. Structure of complex **2** showing the coordination sphere around Mn atom and the atom-numbering scheme. Two $Mn_2(\mu\text{-}COO)_2$ and two $Mn_2(\mu\text{-nicotinate-N,O})_2$ moieties are around the Mn site with Mn···Mn separations of 4.917 Å and 7.342 Å, respectively. The atoms are drawn at a 30% probability level.

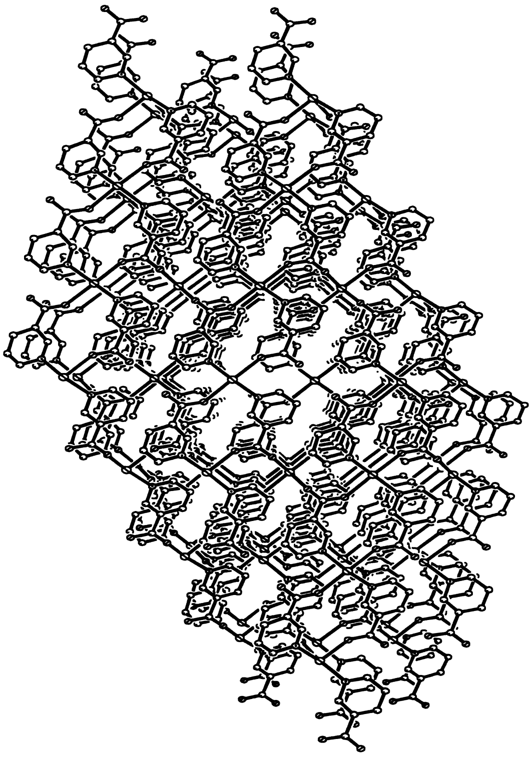

Fig. 3. Packing diagram of unit cell of **2** shows 3-D network structure.

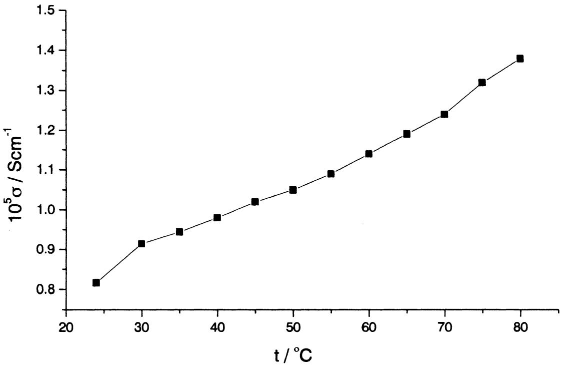

Fig. 4. Plot of temperature-dependent conductance of complex **1**.

largest deviation of ±0.171 Å from the least-squares plane. Around each the manganese site, two $Mn_2(\mu\text{-}COO)_2$ and two $Mn_2(\mu\text{-nicotinate-N,O})_2$ moieties construct a distorted octahedral coordination environment as shown in Fig. 2 with dihedrals of 79.2° between both the $Mn_2(\mu\text{-}COO)_2$ moieties and 64.2° between both $Mn_2(\mu\text{-nicotinate-N,O})_2$. The dihedrals between the $Mn_2(\mu\text{-}COO)_2$ and $Mn_2(\mu\text{-nicotinate-N,O})_2$ moieties are 11.3° and 71.0°. These moieties extend in space and cross to each other to form 3-D network (Fig. 3). This structure makes complex **2** undissolvable in a variety of inorganic and organic solvents.

The IR spectrum of complex **1** displays asymmetric stretching vibrations for the COO^- groups at 1543–1610 cm^{-1} and symmetric stretching vibrations at 1392–1477 cm^{-1} with the differences between the two stretchings, $\Delta(\nu_{as}-\nu_s)$ = ca. 150 cm^{-1}. It is noted that the carboxyl groups in **1** contain both chelating and symmetrical bridging coordination modes, which generally associate with a smaller $\Delta(\nu_{as}-\nu_s)$ value ($<$ 200 cm^{-1}).[7] Compared with complex **2**, which contains the carboxyl groups coordinating to the Mn(II) ions in the bridging mode, it is reasonable to see that complex **2** has a larger $\Delta(\nu_{as}-\nu_s)$ value than complex **1**. In fact, the IR spectrum of complex **2** displays ν_{as} of 1566–1601 cm^{-1} and ν_s of 1389–1417 cm^{-1} with a difference value of $\Delta(\nu_{as}-\nu_s)$ = 180 cm^{-1}. This observation is consistent with the general rule that $\Delta_{\text{chelating}} < \Delta_{\text{bridging}}$.[7,8]

Variable-temperature conductances (σ) of powdered sample of complex **1** were determined in the range from 24 °C (8.16×10^{-6} S cm^{-1}) to 80 °C (1.38×10^{-5} S cm^{-1}); and the temperature dependence of the electrical conductivity is shown in Fig. 4. The value of the conductance and its rising with the rising of temperature display a semiconductor feature of the compound.[9] However, the conductivity of **2** is far from the conductance range ($< 10^{-12}$ S cm^{-1}) of a semiconductor, showing an insulator feature.

Variable-temperature magnetic susceptibility measurements were performed from 300 to 4 K for **1** and **2**. At room temperature, the effective magnetic moment (μ_{eff}) values were determined to be 6.01 BM (**1**) and 5.92 BM (**2**), which are slightly larger or equal to the expected value for an independent spin of $S = 5/2$ (5.92 BM). The $\chi_M T$ values smoothly decrease with the decrease of the temperature in the measured range as shown in Fig. 5, indicating an antiferromagnetic spin-exchange interaction in the two complex molecules. In view of the structures of the two complexes, there are two possible exchange pathways: through extended μ-dicarboxylato (or μ-nicotinato-N,O) ligand bridges and through carboxyl μ-COO bridges. According to the dissimilar chain structures of the two compounds, two models were adopted to give a good fit for their magnetic data.

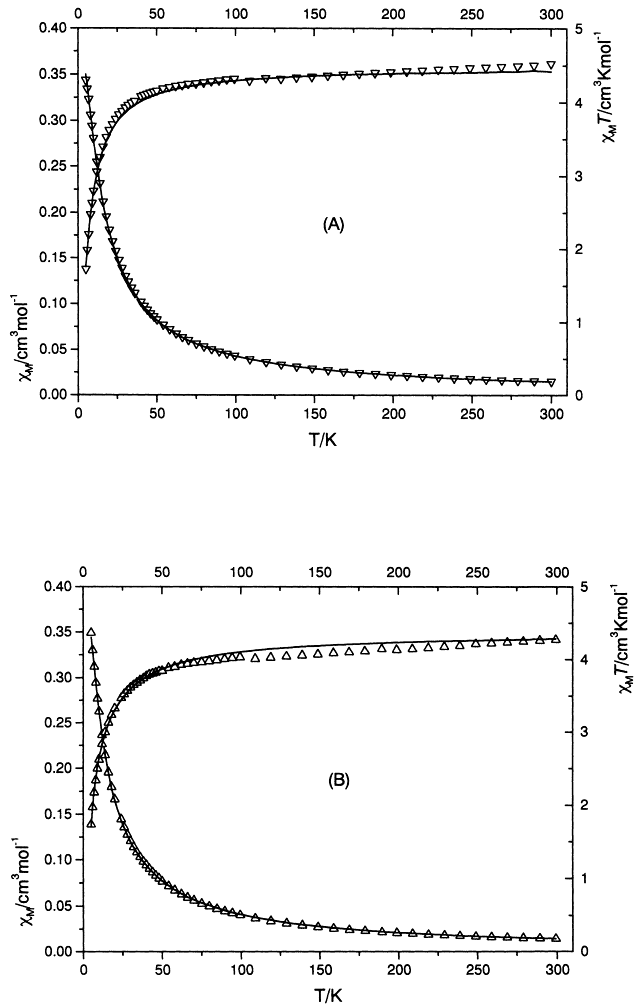

Fig. 5. Temperature dependences of susceptibilities (χ_M) and $\chi_M T$ for complexes **1** (A) and **2** (B). The solid lines represent the calculated values.

Complex **1** has an alternating chain structure (Fig. 1) composed of $Mn_2(\mu\text{-COO})_2$ (J_1) and $Mn_2(\mu\text{-phth})_2$ (J_2) moieties. Equation 1 for a homonuclear alternating chain was used while referring to the literature.[10]

$$\chi = \frac{Ng'^2\mu_B^2}{3kT}\left(\frac{1 + u_1 + u_2 + u_1u_2}{1 - u_1u_2}\right), \tag{1}$$

where $u_1 = Coth(\frac{J'_1}{kT}) - (\frac{kT}{J'_1})$, $u_2 = Coth(\frac{J'_2}{kT}) - (\frac{kT}{J'_2})$,

$J'_i = J_iS(S + 1)$ (i = 1, 2), and $g' = g[S(S + 1)]^{1/2}$.

A least-squares fitting of the experimental data led to $J_1 = -0.942$ cm^{-1}, $J_2 = 0.096$ cm^{-1} and $g = 2.026$. The agreement factor, defined as $R = \Sigma[(\chi_M T)^{cal} - (\chi_M T)^{obsd}]^2/\Sigma[(\chi_M T)^{obsd}]^2$ is 1.49×10^{-4}, exhibiting weak antiferro- and ferro-magnetic interactions in the $Mn_2(\mu\text{-COO})_2$ and the $Mn_2(\mu\text{-phth})_2$ moieties, respectively.

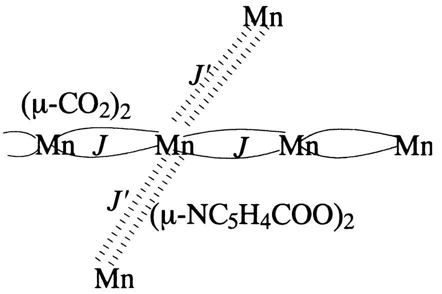

Scheme 2. Magnetic interaction model contains $Mn_2(\mu\text{-CO})_2$ and $Mn_2(\mu$-nicotinate-N,O$)_2$ chains crossing to each other for complex **2**.

The structure of complex **2** consists of two types of chains across each other, which contain $Mn_2(\mu\text{-CO}_2)_2$ and $Mn_2(\mu$-nicotinate$)_2$ units, respectively, as shown in Fig. 3 and Scheme 2. Equation 2 for a homonuclear chain[11] was adopted to treat the interaction in the $Mn_2(\mu\text{-CO}_2)_2$ chains with J representing the interaction between neighboring magnetic species,

$$\chi_{chain} = \left(\frac{Ng^2\mu_B^2}{kT}\right)[A + Bx^2][1 + Cx + Dx^3]^{-1}, \tag{2}$$

where $A = 2.9167$, $B = 208.04$, $C = 15.543$, $D = 2707.2$, and $x = |J|/kT$.

Subsequently, a molecular field approximation[12] was used to contain the $Mn_2(\mu$-nicotinate-N,O$)_2$ chains which cross with the aforementioned $Mn_2(\mu\text{-CO}_2)_2$ chains with interchain interactions of ZJ'. The Z value is the number of nearest magnetic species around a given magnetic site in the crystal lattice.

$$\chi_M = \frac{\chi_{chain}}{[1 - \chi_{chain}(2ZJ'/Ng^2\mu_B^2)]} \tag{3}$$

On this basis, a least-squares fitting of the experimental data led to $J = -0.26$ cm^{-1}, $ZJ' = -0.02$ cm^{-1}, $g = 2.00$ and $R = 5.62 \times 10^{-5}$, exhibiting that antiferromagnetic interactions are present in the system. For the complexes reported in this work, the J values are in the usual range of the caboxylate manganese(II) complexes,[4,5,13] in which the μ-COO and μ-acidate ligand bridges link the Mn(II) sites. Weak antiferro- and ferromagnetic couplings were usually observed in these reported systems, especially, the weak ferromagnetic contribution sometimes occurs from a long pathway via the benzene ring of the phthalate ligands[4b] or the μ-OCO bridges.[4e] In complex **1**, the weak ferromagnetic interaction occurs in $Mn_2(\mu\text{-phth})_2$ moieties, being a long pathway interaction. It is noted that the coordination distortion of the Mn(II) site from a regular octahedron makes the two carboxyl groups of isophthalate to be not coplanar (dihedral of 31° between both COO planes), and may reduce the overlap integral between the magnetic orbitals.[14] Thus, a weak ferromagnetic behavior through the long pathway of isophthalate ligands may not be completely ruled out, though the interaction is very weak. A better coplanarity was observed in the $Mn_2(\mu\text{-COO})_2$ moieties of **1** and both of the $Mn_2(\mu$-nicotinate-N,O$)_2$ and $Mn_2(\mu\text{-COO})_2$ moieties of **2**. This would be favorable to increase the overlap integral for the magnetic orbitals, and antiferromagnetic interactions would be expected. However, the weak magnetic interactions for these two complexes should be attributed to the long separation (4.58–7.34 Å) between the manganese sites. Obviously, owing to the shortening of the Mn···Mn separation, stronger magnetic interactions in the $Mn_2(\mu\text{-COO})_2$ moieties are observed than those in the $Mn_2(\mu\text{-isophth})_2$ or in the $Mn_2(\mu$-nicotinate$)_2$ moieties, implying that the magnetic coupling pathway can be better afforded by μ-carboxyl bridges than μ-isophthalate (for **1**) or μ-nicotinate-N,O (for **2**) bridges.

Experimental

All manipulations were performed under aerobic conditions with materials used as received. IR spectra were recorded by a Bio-Rad FTS-40 Model spectrophotometer. Variable-temperature magnetic susceptibilities were measured on a Model CF-1 superconducting extraction sample magnetometer with a crystal sample kept in a capsule at 5–300 K. Diamagnetic corrections were made with Pascal's constants. Electrical conductivities were determined with pressed pellets on a ZL5-LCR conductometer. Elemental analyses were performed using a Vario EL IIIElemental Analyzer.

[{Mn(*m*-phth)(py)$_2$}$_n$] (1). Isophthalic acid (0.332 g, 2.00 mmol) was dissolved in 30 cm^3 of MeOH/H$_2$O (v/v 1:4). To the solution MnCl$_2$·4H$_2$O (0.397 g, 2.00 mmol) was added and stirred for 3 h at the reflux temperature, resulting in white precipitates being deposited. Then pyridine was added drop-wise (ca. 5 cm^3) until the precipitates dissolved. After stirring for 4h, the solution was allowed to stand for several days at room temperature, affording 0.25 g (yield 33.1%) of block crystals of **1**. Anal. Calcd for $C_{36}H_{28}Mn_2N_4O_8$: C, 57.30; H, 3.74; N, 7.43; Mn, 14.56%. Found: C 57.12; H 3.54; N 7.37; Mn, 14.7%. IR (KBr pellet) 1610, 1568, 1543 for $\nu_{asym}(CO_2)$, 1477, 1444, 1392 cm^{-1} for $\nu_{sym}(CO_2)$.

[{Mn(3-C$_5$H$_4$NCOO)$_2$}$_n$] (2). A mixture slurry composed of MnCl$_2$·4H$_2$O (0.198 g, 1.00 mmol) and nicotinic acid (0.346 g, 2.81 mmol) in 10 cm^3 of H$_2$O was sealed into a teflon tube and heated for 3 days at 160 °C under autogenous pressure. The resulting solid phase consisting of light-red prisms of the complex was filtered and dried at room temperature, affording 0.15 g (yield 50.1%) of **2**. Anal. Calcd for $C_{12}H_8MnN_2O_4$: C, 48.16; H, 2.68; N, 9.36; Mn, 18.39%. Found: C 47.86; H 2.61; N 9.62; Mn, 17.91%. IR (KBr pellet) 1601, 1566 for $\nu_{asym}(CO_2)$, 1417, 1389 cm^{-1} for $\nu_{sym}(CO_2)$.

Crystallography. Intensity data for single crystals of the two complexes were collected on a Siemens Smart CCD diffractometer. The structures were solved by a combination of direct methods and Fourier techniques and refined anisotropically by full-matrix least-squares on F^2 for the two compounds.[15] Hydrogen atoms were geometrically located and added to the structure factor calculations, but their positions were not refined. For **1**, the final refinement included 216 variable parameters for 2573 ($I > 2\sigma(I)$) reflections, and converged to $R = 0.0383$ and $R_w = 0.1066$ with the highest and minimum residual peaks of 0.596 and -0.707 e/Å^3. For **2**, 87 variable parameters and 835 ($I > 2\sigma(I)$) reflections were refined to give final $R = 0.0437$ and $R_w = 0.1166$ with residual peaks of 0.525 and -0.434 e/Å^3. Crystal data and structure refinements are summarized in Table 2. The CIF data for two crystals are deposited as Document No. 75055 at the Office of the Editor of Bull. Chem. Soc. Jpn. The non-hydrogen atom coordinates and anisotropic thermal parameters, bond distances and angles, and the coordinates of the hydrogen atoms have been deposited (Nos. CCDC 173334 and 173333 for **1** and **2**, respectively) at the Cambridge Crystallographic Data Centre, 12 UnionRoad, Cambridge CB2 1EZ, UK.

This work was supported by NNSFC (No. 30170229 and 29973047), the State Key Basic Research and Development Plan of China (G1998010100), and Expert Project of Key Basic Research from Ministry of Sci&Tech.

Table 2. Summary of Crystal Data for the Complexes **1** and **2**

	1	**2**
Formula	$C_{18}H_{14}N_2O_4Mn_1$	$C_{12}H_8Mn_1N_2O_4$
M_r	377.25	299.14
Crystal system	Triclinic	Monoclinic
Space group	*P*-1	*C*2/*c*
a/Å	9.0271(2)	14.7930(12)
b/Å	9.6678(3)	9.6011(8)
c/Å	10.2360(3)	8.7631(7)
α/°	75.732(1)	
β/°	73.658(1)	114.229(2)
γ/°	87.958(1)	
V/Å^3	830.24(4)	1134.98(16)
Z	2	4
ρ_{calc}/g cm^{-3}	1.509	1.751
μ(Mo $K\alpha$)/cm^{-1}	0.820	1.174
T/K	293(2)	293(2)
Unique reflections	2573 ($I > 2\sigma(I)$)	835 ($I > 2\sigma(I)$)
R_1[a], wR_2[b]	0.0383, 0.1066	0.0437, 0.1166
R_1, wR_2 (all data)	0.0432, 0.1093	0.1166, 0.0543

a) $R = \Sigma||F_o| - |F_c||/\Sigma|F_o|$. b) $R_w = [\Sigma w(|F_o| - |F_c|)^2/\Sigma wF_o^2]^{1/2}$ **1**: $w = 1/[S^2(F_o^2) + (0.0568P)^2 + 0.0876P]$, where $P = (F_o^2 + 2F_c^2)/3$. **2**: $w = 1/[S^2(F_o^2) + (0.1000P)^2 + 0.0000P]$, where $P = (F_o^2 + 2F_c^2)/3$.

References

1 a) F. Serpaggi and G. Ferey, *J. Mater. Chem.*, **8**, 2737 (1998). b) D. W. Bruce and D. O'Hare, "Inorganic Materials," 2nd ed, Wiley (1996). c) M. J. Plater, M. R. St. J. Foreman, E. Coronado, C. J. Gomez-Garcia, and A. M. Z. Slawin, *J. Chem. Soc., Dalton Trans.*, **1999**, 4209. d) B. Paluchowska, J. K. Maurin, and J. Leciejewicz, *J. Coord. Chem.*, **51**, 335 (2000).

2 a) N. A. Law, M. T. Caudle, and V. L. Pecoraro, *Adv. Inorg. Chem.*, **46**, 305 (1998). b) V. K. Yachandra, K. Sauer, and M. P. Klein, *Chem. Rev.*, **96**, 2927 (1996). c) C. Tommos and G. T. Babcook, *Acc. Chem. Res.*, **31**, 18 (1998).

3 a) G. Christou, *Acc. Chem. Res.*, **22**, 328 (1989). b) W. Wernsdorfer, N. Aliaga-Alcalde, D. N. Hendrickson, and G. Christou, *Nature*, **416**, 406 (2002). c) B. Albela, M. S. El Fallah, J. Ribas, K. Folting, G. Christou, and D. N. Hendrickson, *Inorg. Chem.*, **40**, 1037 (2001). d) A. R. Schake, J. B. Vincent, Q. Li, P. D. W. Boyd, K. Folting, J. C. Huffman, D. N. Hendrickson, and G. Christou, *Inorg. Chem.*, **28**, 1915 (1989). e) S. Wang, K. Folting, W. E. Streib, E. A. Schmitt, J. K. McCusker, D. N. Hendrickson, and G. Christou, *Angew. Chem., Int. Ed. Engl.*, **30**, 305 (1991). f) S. Wang, J. C. Huffman, K. Folting, W. E. Streib, E. B. Lobkovsky, and G. Christou, *Angew. Chem., Int. Ed. Engl.*, **30**, 1672 (1991). g) R. J. Kulawiec, R. H. Crabtree, G. W. Brudvig, and G. K. Schulte, *Inorg. Chem.*, **27**, 1309 (1988).

4 a) J. W. Bats, A. Kallel, and H. Fuess, *Acta Crystallogr., Sect. B*, **34**, 1705 (1978). b) C. S. Hong and Y. Do, *Inorg. Chem.*, **36**, 5684 (1997). c) C. S. Hong and Y. Do, *Inorg. Chem.*, **37**, 4470 (1998). d) Y. Zhang, J. Li., M. Zhu, Q. Wang, and X. Wu, *Chem. Lett.*, **1998**, 1051. e) X. S. Tan, J. Sun, D. F. Xiang, and W. X. Tang, *Inorg. Chim. Acta*, **255**, 157 (1997). f) X. S. Tan, D. F. Xiang, W. X. Tang, and K. B. Yu, *Polyhedron*, **16**, 1411 (1997). g) M. R. Bermejo, M. Fondo, A. Garcíia-Deibe, A. M. González, A. Sousa, J. Sanmartín, C. A. McAuliffe, R. G. Pritchard, M.

Watkinson, and V. Lukov, *Inorg. Chim. Acta*, **293**, 210 (1999).

5 a) V. Tangoulis, G. Psomas, C. Dendrinou-Samara, C. P. Raptopoulou, A. Terzis, and D. P. Kessissoglou, *Inorg. Chem.*, **35**, 7655 (1996). b) S. O. H. Gutschde, M. Molinier, A. K. Powell, R. E. P. Winpenny, and P. T. Wood, *Chem. Comm.*, **1996**, 823. c) J. Cano, G. De Munno, J. Sanz, R. Ruiz, F. Lloret, J. Faus, and M. Julve, *J. Chem. Soc., Dalton Trans.*, **1994**, 3465.

6 X. Hao, Y.-G. Wei, Q. Liu, and S.-W. Zhang, *Acta Crystallogr., Sect. C*, **56**, 296 (2000).

7 G. B. Deacon and R. J. Philips, *Coord. Chem. Rev.*, **33**, 227 (1980).

8 N. W. Alcock, V. M. Tracy, and T. C. Waddington, *J. Chem. Soc., Dolton Trans.*, **1976**, 2243.

9 C. Kettel, “Solid State Physics,” 5th ed, John Wiley & Sons Inc. New York, (1976).

10 R. Cortés, M. Drillon, X. Solans, L. Lezama, and T. Rojo, *Inorg. Chem.*, **36**, 677 (1997).

11 W. Hiller, J. Strähle, A. Datz, M. Hanack, W. E. Hatfield, L. W. ter Haar, and P. Gütlich, *J. Am. Chem. Soc.*, **106**, 329 (1984).

12 a) C. J. O’Connor, *Prog. Inorg. Chem.*, **29**, 203 (1982). b) M. Handa, Y. Sayama, M. Mikuriya, R. Nukada, I. Hiromitsu, and K. Kasuga, *Bull. Chem. Soc. Jpn.*, **71**, 119 (1998). c) H.-Y. Shen, W.-M. Bu, E.-Q. Gao, D.-Z. Liao, Z.-H. Jiang, S.-P. Yan, and G.-L. Wang, *Inorg. Chem.*, **39**, 396 (2000).

13 Z. H. Jiang, S. L. Ma, D. Z. Liao, S. P. Yan, G. L. Wang, X. K. Yao, and R. J. Wang, *J. Chem. Soc., Chem. Commun.*, **1993**, 745.

14 J. Cano, G. D. Munno, J. L. Sanz, R. Ruiz, J. Faus, F. Lloret, M. Julve, and A. Caneschi, *J. Chem. Soc., Dolton Trans.*, **1997**, 1915.

15 “SAINT and SHELXTL (Version 5.0),” Siemens Analytical X-ray Instruments Inc., Wisconsin, Madison, USA (1994).